Iranian Journal of Astronomy and Astrophysics
Vol. 4, No. 1, Spring 2017

DOI:10.22128/ijaa.2017.106

Iranian Journal of Astronomy and Astrophysics

Modeling Magnetic Field in Heavy ion Collisions Using Two Different Nuclear Charge Density Distributions

Susan Abbas Nejad[1] · Supervisor: Dr. Umut Gürsoy[2]
[1] University College Utrecht, Utrecht, The Netherlands,
email: susanabbasnejad@gmail.com
[2] Department of Physics, Utrecht University, Utrecht, The Netherlands

Abstract. By studying the properties of matter during heavy-ion collisions, a better understanding of the Quark-Gluon plasma is possible. One of the main areas of this study is the calculation of the magnetic field, particularly how the values of conductivity affects this field and how the field strength changes with proper time. In matching the theoretical calculations with results obtained in lab, two different models for charge density distribution inside ions is used. In this study, after explanation of some theoretical background, the magnetic field contribution of the spectators and participants in Pb-Pb ion collision is calculated in a conductive medium and vacuum. Results are compared using two different nuclear charge density models.

Keywords: Quark-Gluon Plasma, QCD, Heavy Ion Collisions, Electromagnetic field, Nuclear density distributions,

1 Introduction

One of the main areas of modern theoretical Physics is the theory of Quantum Chromodynamics (QCD for short). This theory studies the strong force which mainly acts between quarks and gluons. As the name suggests, this plasma is a soup of quarks and gluons. As predicted by this theory, matter at high energy changes into a quark gluon plasma phase. Some theories state that the universe was in this state in the "Quark Epoch", 10^{-12} until 10^{-6} seconds after the big bang [12]. This is also most likely the state of matter at the core of neutron stars [16]. This phase of matter is, thus, very interesting to study.

Since this phase transition is obtained at very high temperatures (thus high energies as well), it can only be obtained on Earth in laboratories like CERN (see figure 1 for a depiction of these experiments). At CERN, this state of matter is obtained by colliding lead ions together at near the speed of light with the nuclei having energies of a few trillion electron-volts each [2]. When two ions are collided together at very high speed, the result will be quark-Gluon plasma (QGP for short) formation for a short period of time (A sketch of the collision is shown in figure 1). Creating this phase of matter at these laboratories helps to study the structure of hadrons at high energy and how the QGP is thermalized. One of the steps in studying this medium is the study of its electromagnetic field. This thesis will focus on the magnetic field in such a collision using two different models describing the nucleon density.

Before describing the theory, it is useful to mention some characteristics of heavy-ion collisions:

1) One of the characteristics of a heavy-ion collision is its centrality. Collisions are mostly not head-on. Figure 1 again shows a sketch of an off-central collision. The center-to-center

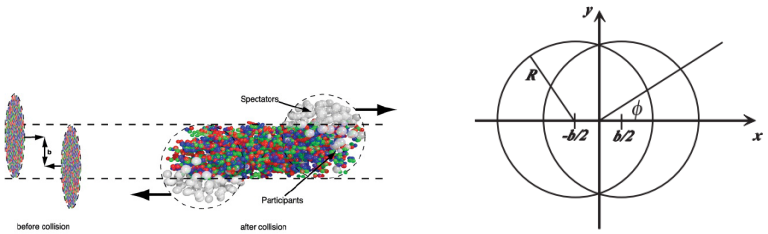

Figure 1: Right: Sketch of an off-central collision. For the spectators one integrates over the two crescent-shaped parts of the two ions and for the participants, one integrates over the almond shaped part in the middle and accounting for both the ion moving in the +z direction and -z direction Left: The set-up of a heavy-ion collision

distance of the two ions is denoted by b. This constant expresses the level of centrality of the collision.

2) As the two ions are travelling at 99.9999 percent the speed of light [4], the ions will be strongly Lorentz contracted (contracted to 1 percent of their original size. See [8]). As a result, in this paper we assume that the neutrons and protons reside on a flat disk as this is an appropriate simplifying approximation.

3) As the collision is not head-on, there are two parts to the collision: the participants (participating in the collision) and the spectators (not participating in the collision) [17]. As seen in figure 1, the participant part of the collision is the area where the two circles meet and the spectators reside on the rest of the area of the two circles (representing ions). In modeling the magnetic field of this plasma, we differentiate between these two parts for reasons which shall be explained. We shall also compare their contribution to the total magnitude of the field. The calculated magnetic field in this thesis will be an interpolated function of proper time. Thus, we will also see how this field changes with time. Before moving on any further, it is helpful to express that we use the Natural Units system in this paper as it is widely used in particle physics. As for the constants used in this thesis, we shall use the constants obtained by measurements taken at the Pb-Pb collision experiments at CERN which started in 2010 [21].

1.0.1 The electromagnetic field of one charge in conductive environment

The environment around a quark gluon plasma has a certain conductivity. As we shall see, this conductivity is such that it is negligible a very short time after the collision but it will affect the magnetic field a very short while afterwards (perhaps as the value of conductivity itself increases).

To find the expression for the Electromagnetic fields in this case, we first take Maxwell's equations with conductivity included. Then, we find the expression for the magnetic field. Knowing the magnetic field at any point in space will also give us the electric field at that point.

Replacing expressions from Maxwell's equations and the expression for Z, we get the equation for the magnetic field:

$$\nabla^2\vec{B} - \frac{\partial^2\vec{B}}{\partial t^2} - \sigma\frac{\partial\vec{B}}{\partial t} = -ev\vec{\nabla}\times(\hat{z}\delta_{(z-vt)}\delta_{(x_\perp - x_\perp)})$$

Since the differential operators here are linear, we can use the method of Green's function to solve for B.

And the B field becomes:

$$eB_y = 2^{\alpha_{em}}\hat{y}\int\int \frac{J_1(bk_\perp)k_\perp^2}{\frac{\omega^2}{\upsilon^2}+k_\perp^2-\omega^2-i\sigma\omega}e^{i\omega(\frac{z}{\upsilon}-t)}d_{k\perp}d_\omega$$

Here, as the particle is moving at a speed very close to the speed of light, we can make the simplifying assumption that $\upsilon = c = 1$. In this case, the magnetic field will be:

$$eB_y = 2\alpha_{em}\hat{y}\int\int \frac{J_1(bk_\perp)k_\perp^2}{k_\perp^2-i\sigma\omega}e^{i\omega(z-t)}d_{k\perp}d_\omega$$

From here, we proceed first by solving the integral over omega. This integral can be solved using the residue theorem from complex analysis. According to this theorem, the integral of a function over a closed curve is:

$$\int f_{(z)}d_z = 2\pi i\Sigma Res(f,a_k)$$

Where a_k are the poles of the function. Here, there is only one pole at $\frac{k_\perp^2}{i\sigma} = \omega$. So, we get:

$$\int \frac{e^{(i\omega(z-t))}}{i\sigma(\frac{k_\perp^2}{i\sigma}-\omega)}d_\omega = 2\pi i\Sigma Res(f,a_k=\frac{k_\perp^2}{i\sigma})$$

Where the residue is:

$$\text{Res(f,a}_k = \tfrac{k_\perp^2}{i\sigma}) = Lim\ \underset{\omega\frac{k_\perp^2}{i\sigma}}{\rightarrow} \frac{e^{i\omega(z-t)}}{i\sigma} = \tfrac{1}{i\omega}e^{i\frac{k_\perp^2}{i\sigma}(z-t)}$$

So, the integral becomes:

$$eB_y = \frac{4\pi\alpha_{em}}{\sigma}\hat{y}\int J_1(bk_\perp)e^{\frac{k_\perp^2}{\sigma}(z-t)}k_\perp^2 dk_\perp$$

The integral over $k_\perp$ can be evaluated analytically:

$$eB_y = \hat{y}\frac{\alpha_{em}b\sigma}{2(t-z)^2}e^{\frac{b^2}{e^{4(t-z)}}}$$

However, for a more accurate calculation, we take $\upsilon \neq 1$. Thus, in this case we have:

$$eB_y = \frac{\alpha_{em}}{\pi}\hat{y}\int J_1(bk_\perp){k_\perp}^2 dk_\perp \int \frac{e^{i\omega(\frac{z}{\upsilon}-t)}}{\frac{\omega^2}{\upsilon^2}+k_\perp^2-\omega^2-i\sigma\omega}d\omega$$

$$eB_y = \frac{\alpha_{em}}{\pi}\hat{y}\int J_1(bk_\perp)k_\perp^2 d_{k\perp}\int \frac{e^{i\omega(\frac{z}{\upsilon}-t)}}{\frac{\omega^2}{\upsilon^2}+k_\perp^2-\omega^2-i\sigma\omega}d_\omega$$

In this case, we have two poles:

$$\omega_\pm = \frac{i\sigma\lambda^2\upsilon^2}{2}(1\pm\sqrt{1+\frac{4k_\perp^2}{\sigma^2\lambda^2\upsilon^2}})$$

Here, we pick only the ω_- part as with the other one, the function for B would diverge. Picking ω_- and calculating the residue for this pole, we get for the field:

$$eB_y = \frac{\alpha_{em}}{\pi}\hat{y}\int \frac{J_1(bk_\perp)k_\perp^2 e^{(-\omega_-(\frac{z}{\upsilon}-t))}}{\sigma(1+\frac{4{k_\perp}^2}{\sigma^2\lambda^2\upsilon^2})^{1/2}}d_{k\perp}$$

To calculate the integral, we first change the variables in the following way:

$$u = (1+\frac{4{k_\perp}^2}{\sigma^2\lambda^2\upsilon^2})^{1/2} \qquad \frac{du}{dk_\perp} = \frac{1}{u}\frac{4k_\perp}{\sigma^2\lambda^2\upsilon^2}$$

$$u^2-1 = \frac{4{k_\perp}^2}{\sigma^2\lambda^2\upsilon^2} \qquad k_\perp = \frac{\sigma\lambda\upsilon}{2}\sqrt{u^2-1} \qquad dk_\perp = u(\frac{\sigma^2\lambda^2\upsilon^2}{4k_\perp})du$$

So, the field becomes:

$$eB_y = \frac{\alpha_{em}}{\pi}\hat{y}\int \frac{2J_1\frac{b\sigma\lambda\upsilon}{2}\sqrt{u^2-1}(\frac{\sigma^2\lambda^2\upsilon^2}{4})^2\sqrt{u^2-1}}{\sigma^2\lambda\upsilon}e^{-\frac{\sigma\lambda^2\upsilon^2}{2}(1-u)(t-\frac{z}{\upsilon})}du$$

Putting the constant terms to the left side of the integral:

$$eB_y = \frac{\alpha_{em}}{2\pi}[\frac{b\sigma^3\lambda^4\upsilon^4}{8}e^{-\frac{\sigma\lambda^2\upsilon^2}{2}(t-\frac{z}{\upsilon})}]\int J_1(\frac{b\sigma\lambda\upsilon}{2}\sqrt{u^2-1})\sqrt{u^2-1}e^{-\frac{\sigma\lambda^2\upsilon^2}{2}(t-\frac{z}{\upsilon})u}du$$

Now, we have the B field in terms of the normal variables (x, y, z, t) and υ. However, there is a more convenient coordinate system to describe heavy ion collisions. That system uses τ (proper time) , η (pseudo-rapidity) , $x_\perp$ (distance from the center of the ion to where we want to find the field) and ϕ (angel from x axes to the line of $x_\perp$).

Pseudo-rapidity in natural units is a dimension-less coordinate which is similar to a hyperbolic angel [21]. In this system of coordinates, instead of using speed, we use a similar constant related to speed called rapidity Y. These variables are the experimental observables in heavy ion collision experiments and thus are more convenient to work with [18]. The transformations from Cartesian coordinates to the new coordinates are as follows:

$$\tau = \sqrt{t^2-z^2} \qquad \eta = arctanh(\frac{z}{t}) \qquad x_\perp = \sqrt{x^2+y^2}$$

$$\varphi = acrtan(y/x) \qquad Y = arctanh(\frac{\upsilon_z}{C}) \qquad z' = \beta t$$

And the other way:

$$t = \tau Cosh(\eta) \qquad x = x_\perp Cos(\varphi) \qquad y = x_\perp Sin(\varphi)$$

$$z = \tau sinh(\nu) \qquad \upsilon = tanh(Y)$$

At this stage, one should consider taking into account the correct range for the variables. As it can be seen, $\eta = 0$ corresponds to the t-axis and $\eta = \pm\infty$ corresponds to the light cone $(z = t)$. As the results do not depend on the pesudo-rapidity window in which we initialize the particles (as long as it is larger than the observed rapidity bins), for most studies, the ammount $-3 < \eta < 3$ is sufficient [3]. This value is also within the window of pseudo-rapidity calculations in ALICE [22]. For rapidity, we also use the value $Y_0 \simeq 7.6$ used in the

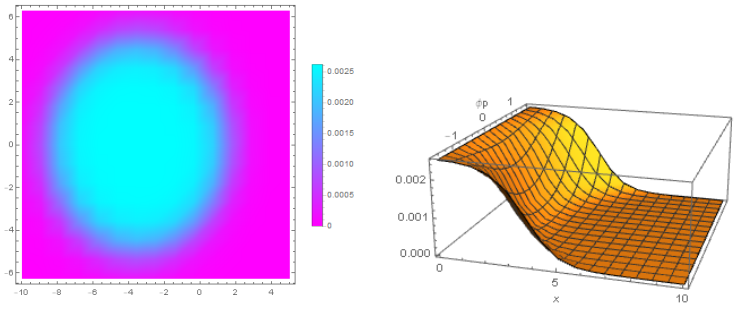

Figure 2: Right: Plot of the number density function (equation 2.1) for Woods-Saxon model in termsof x and y for lead ion the center of which is positioned at $x_{\perp 0} = 3.5$. The Plot-Legendon the right shows the relative value for the number density function for the correspondingcolour. As we can see here, the density is highest at the center and lowest as we go to theborders of the ion as expected.Left: 3D plot of the number density as a function of $x'_{\perp}$ and ϕ'. It is visible that along a constang angel, as x increases, the number density decreases. This drop in density is similar to the drop in Woods-Saxon potential as a function of x; as expected.

LHC experiments [1]. As for τ, we use the proper time until the time of thermalization. It is known that the proper time of thermalization is about 0.5 fm [23].

This integral can again be calculated analytically:

$$eB_y = \frac{2\pi(\lambda^2\sigma^2 v^2)}{4}\frac{\lambda v}{2}e^{(t-\frac{z}{v})\frac{\sigma\lambda^2 v^2}{2}}\sqrt{\frac{2}{\pi}}\beta(\alpha^2+\beta^2)^{-3/4}K_{3/2}(\sqrt{\alpha^2+\beta^2})$$

Where

$$K_{3/2}(z) = \frac{2}{\pi}e^{-z(1+\frac{1}{z})}$$

1.1 Coordinate transformations:

The magnetic field in terms of the new variables is:

$$eB_y^+(\tau,\eta,x_\perp,\phi) = \alpha\sinh(Y_b)(x_\perp\cos\phi - x'_\perp\cos\phi')\frac{(\frac{|\sinh(Y_b)|}{2}\sqrt{\Delta}+1)}{\Delta^{\frac{3}{2}}}e^A\,,$$

where $\alpha = e^2/(4\pi)$ is the electromagnetic coupling constant, $Y_b \equiv (\beta)$ is the rapidity of the particle moving in the +z direction. We have also defined:

$$A = \frac{\sigma}{2}(\tau\sinh(Y_b)\sinh(Y_b-\eta) - |\sinh(Y_b)|\sqrt{\Delta}$$

$$\Delta = \tau^2\sinh^2(Y_b-\eta) + {x_\perp}^2 + (x'_\perp)^2 - 2\times x_\perp\times x'_\perp\times\cos(\phi-\phi')$$

We only take into account the y component of the field since we will be studying the field evolution at around the center where this component is the main component of the field as also stated by [8]. Knowing the Magnetic field, one can find the Electric field as follows:

$$eE_x^+(\tau,\eta,x_\perp,\phi) = eB_y^+(\tau,\eta,x_\perp,\phi)\coth(Y_b-\eta)\,.1.4$$

So now we have the x,y and z part of the Electric and magnetic field for one moving particle in lab frame (calculations also carried out by [1] , [20]).

2 Numerical Integration

At this stage, we have the contribution to the magnetic field for only one particle. Our aim is to integrate over the contributions of the field from all the particles on the 2D ion discs (see figure 2).

As we will see later, the integral, when found, will be a function of $(\eta, \tau, \phi, x_\perp)$. This integral cannot be found analytically as it is too complicated. Hence, we use numerical integration to find a good approximation to the integral.

In this section, we discuss the assumptions and models used to do this integration. First, two different models for particle distribution functions inside the ions are introduced. Afterwards some theories regarding relations with proper time are discussed. Finally, the magnetic field is calculated using the two models and the results are compared.

2.1 Two Different Nuclear Distribution Function Models

To find the magnetic field of the moving ion, we have to add up the contributions due to all the particles (see figure 1). For this purpose, we use two different models for distribution of protons inside the nuclei. As we shall see, the hard-sphere distribution is more simplified than the Woods-Saxon distribution which may be unrealistic in some situations. Thus, in following the numerical calculation of the magnetic field, we use both these distributions to compare them with previously obtained results.

2.1.1 The Woods-Saxon Model

The more accurate of the two nuclear Distribution Function models is called the Woods-Saxon model where the number density of protons is given by the equation bellow (see also [24] and [1]):

$$n_A(r) = \frac{n_0}{1 + e^{\frac{r-R}{d}}} 2.1$$

Where R is the radius of the nuclei and r is the distance from the center of nuclei. The values for constants are $n_0 = 0.17fm^{-1}$ and $d = 0.54fm$ and $R = 7fm$. The distance from the center of nuclei in terms of the x-y-z coordinates is:

$$r_\pm = \sqrt{(x \pm \frac{b}{2})^2 + y^2 + z^2}$$

Switching to the new coordinate system:

$$r_\pm = \sqrt{(x'_\perp \pm bx'_\perp Cos(\phi')) + \frac{b^2}{4} + (z - \tau^2 Sinh^2(\eta))}$$

Figure 3 shows some plots of the number density function (2.1):

To get the density at any ($x_\perp$, ϕp), we integrate over z (see the integral bellow). The reason for the original z-dependence is due to the uncertainty in the position of each particle along the z direction.

$$\rho_\pm(x'_\perp) = \frac{1}{N} \int dz' \frac{n_0}{1 + e^{\frac{r-R}{d}}} 2.2$$

Where N is the normalization factor. The values for constants are $n0 = 0.17fm^{-3}$ and $N = 1.6487$ and $d = 0.54fm$. This integral is also of the type which cannot be evaluated analytically and a numerical calculation must be done to evaluate a near-enough approximation.

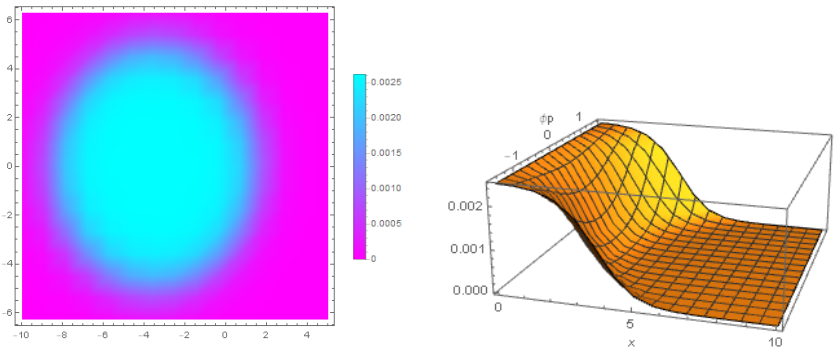

Figure 3: Right: 3D plot of the number density as a function of $x'_\perp$ and ϕ'. It is visible that along a constang angel, as x increases, the number density decreases. This drop in density is similar to the drop in Woods-Saxon potential as a function of x; as expected. Left: Plot of the number density function (equation 2.1) for Woods-Saxon model in terms of x and y for lead ion the center of which is positioned at $x_{\perp 0} = 3.5$. The Plot-Legend on the right shows the relative value for the number density function for the corresponding colour. As we can see here, the density is highest at the center and lowest as we go to the borders of the ion as expected.

2.1.2 Hard-Sphere Model

Another model for the density function of charges within an ion is the Hard-Sphere model which is more simplified and easier to work with:

$$\rho_\pm(x'_\perp) = \frac{3}{2\pi R^3}\sqrt{R^2 - (x'_\perp \pm bx'_\perp Cos(\phi')) + \frac{b^2}{4}} 2.3$$

2.2 A Note on Proper Time

One way to follow the numerical integration is to do so on the freeze-out surface. This surface is a hyper-surface in space-time where hadrons are produced during the collision as the matter cools down which is defined by a function $\tau_{freeze[x_\perp]}$ [21]. Calculation of the magnetic field on this surface decreases the number of variables by one.

Another way, however, is to integrate for the magnetic field at any point in space-time and not just the freeze-out surface. This way requires more computation time but is more accurate.

2.3 Spectator Contribution

At this point, one has to differentiate between the spectators and the participants when doing the numerical integration. For the spectator contribution, the amount of rapidity does not change (the particles are not participating in any reaction and are assumed to move with constant speed before and after the collision), but for the participants, it does change. In our case for Pb-Pb collisions with center-of-mass energy per nucleon pair of about 2 TeV, we take $Y0 \equiv 7.6$ [22]. For the spectator contribution, we only integrate over $x'_\perp$ and ϕ' as follows [1]:

$$\Sigma eB_{s,y} = -Z\int_{-\frac{\pi}{2}}^{\frac{\pi}{2}} d\phi' \int_{x_{in}}^{x_{out}} \rho_\pm(x'_\perp)\theta_\pm(x_\perp)(1-\theta_\mp(x_\perp))eB_i x_\perp dx'_\perp$$

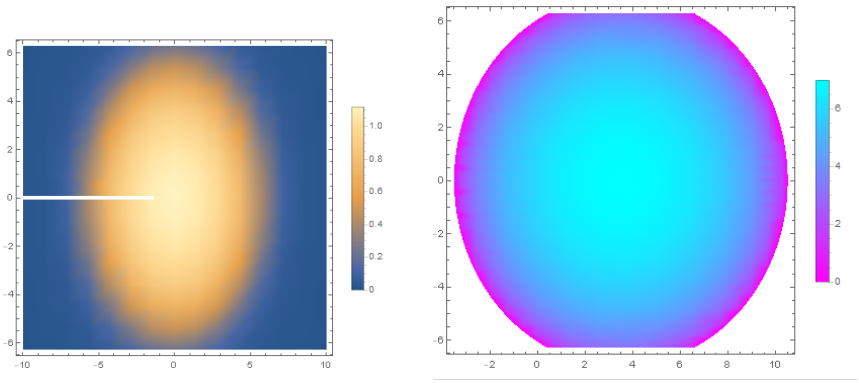

Figure 4: Left: Density plot of the Integrated density function (equation 2.2) for Woods-Saxon model. The integral is approximated by numerical integration (see Appendix) and a function $\rho_{(x_\perp,\phi')}$ is obtained by interpolation. Right: the density-plot of the density function for Hard-Sphere model in terms of x and y for lead ion. The Plot-Legend on the right show the relative value for the density function for the corresponding colour. It is observed that the density is highest at the center and lowest as we go to the borders, exactly as one would expect to get with a sphere of uniformly distributed matter. However, as this model is more simplified, it also looks more symmetric and perfect which may be an unrealistic model in some situations.

Where $\rho_\pm(x'_\perp)$ describes the particle distribution function for a relativistic ion and $\theta_{-(x_\perp)} = \theta[R^2 - (x_\perp - \frac{b}{2}\hat{x})^2]$. We use $Z = 82$ as it is the atomic number for Lead nuclei which is used in heavy ion collisions at CERN. Here, x_{in} and x_{out} describe the crescent shaped loci where we find the particles which are either moving in the +z or -z direction but not both and are described by the following functions [1]:

$$x_{in/out}(\phi') = \mp\frac{b}{2}cos(\phi') + \sqrt{R^2 - \frac{b^2}{4}sin^2(\phi')}$$

The θ functions account for charges moving in the opposite directions. Replacing these functions by the magnetic field as a function of $\phi, \eta, x'_\perp, \tau$ (moving in +z direction) and $\pi - \phi, -\eta, x'_\perp, \tau$ (moving in -z direction) we get:

$$eB^-_{s,y} = -Z\int_{-\frac{\pi}{2}}^{\frac{\pi}{2}} d\phi' \int_{x_{in}}^{x_{out}} x'_\perp \rho_+(x'_\perp)((eB^+_y(\pi - \phi, -\eta, x'_\perp, \tau)) + (eB^+_y(\phi, \eta, x'_\perp, \tau)))dx'_\perp$$

3 Results

3.0.1 Spectator Contribution with The Hard-Sphere Model

For the particle distribution function, we first use the hard-sphere model which is easier to work with. This has been done before by [1] and is done here for comparison. Figure 5 bellow shows the results of the numerical calculation using the density function shown in formula (2.3), with and without conductivity:

It is clear from the figure that the field is very strong at low values of τ . In the short moments before/during/after the impact of two ions in non-central collisions, there is a very strong magnetic field in the reaction zone [5]. In fact, being of order of 10^{18} Gauss, these fields are among the strongest magnetic fields in nature [3].

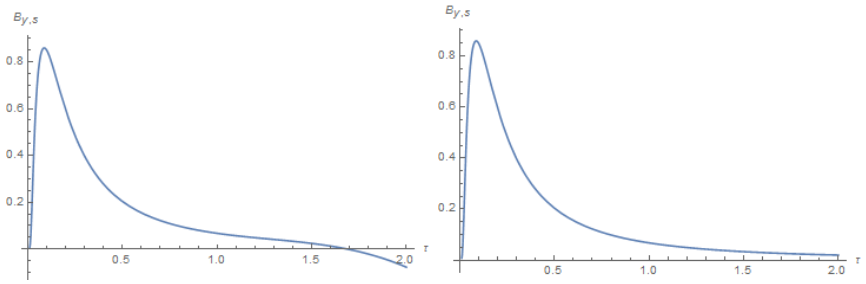

Figure 5: Right: Plot of the interpolated function of B in terms of τ at ($xp = 0.001$, $\phi = \frac{\pi}{2}$, $\eta = 0.1$) with the exception of having non-zero conductivity ($\sigma = 0.023$). Again, results are similar enough to [1]. Left: Plot of the interpolated function of total B field in terms of τ at ($xp = 0.001$, $\phi = \frac{\pi}{2}$, $\eta = 0.1$) in medium with zero conductivity. The maximum value of the field is $0.85fm^{-2}$ which, upon conversion gives us 1.7×10^{18} Gauss. As expected, results are similar to [1]. The part of the graph that is negative is a result of extrapolation and shall be ignored.

As can also be seen, these fields decay almost immediately (put the values in seconds). However, including the effects of a conducting medium, the field decays slower (see also [5] and figure 6 bellow).

3.0.2 Spectator Contribution with Woods-Saxon Model

To calculate the field using this model, we use the function obtained by interpolation (described in section 2.1.1). Figure 7 bellow shows the obtained result with conductivity. The maximum value here is about $0.95fm^{-2}$. Compared with the maximum value of about $0.84fm^{-2}$ it shows a higher but close-enough value.

3.0.3 Participants

Unlike the calculation of the B-field for Spectators where the rapidity Y does not change (because they do not collide with particles from the other direction), for the participant contribution to the field, we have to take into account the change in rapidity. Thus, to get the total field we will also integrate over the distribution of Y given by the equation bellow ([8] and [9]).

$$f(Y_b) = \frac{a}{2Sinh(aY_0)} e^{aY_b} 2.4$$

Where $-Y_0 < Y_b < Y_0$ [1] and $Y0 \approx 7.6$ and $a \approx 0.5$. Thus the total field will be [1]:

$$eB_{y,p} = -Z \int_{-Y_0}^{Y_0} f(Y_b) d_{Y_b} \int_{-\frac{\pi}{2}}^{\frac{\pi}{2}} d\phi' \int_0^{x_{in}(\phi')} \rho_{\pm}(x'_{\perp}) \theta_{\pm}(x_{\perp})(1 - \theta_{\mp}(x_{\perp})) eB_i x_{\perp} dx_{\perp}$$

3.0.4 Participants Contribution With The Hard-Sphere Model

As for the participants contribution to the Magnetic field using the Hard-Sphere model,the maximum of the field is only about $0.065fm^{-1}$, i.e. about only a hundredth of the contribution of the spectators. This is mainly due to the fact that there are less particles participating in the collision.

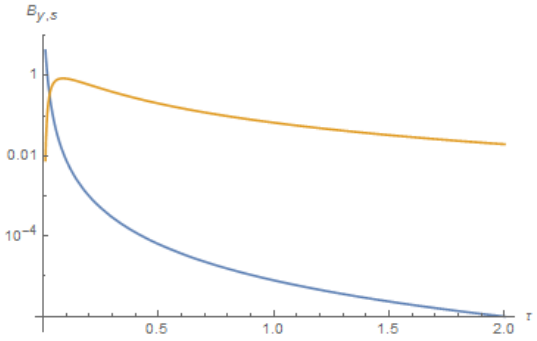

Figure 6: Figures 9 and 10 plotted together. The blue line shows the field without conductivity and the orange line shows the field including conductivity. As can be seen, a conductive medium slows down the decay of the magnetic field. In the very early times, the plot using a medium without conductivity is more accurate as the conducting medium is not formed immediately as quarks take some time to be created from the Glasma field [13]. Also we assumed that the medium does not alter during the evolution of QGP, thus the usage of a constant value for conductivity. However, as also seen from the graph, a decrease in conductivity due to expansion of the medium will only increase the decay speed of the magnetic field [13].

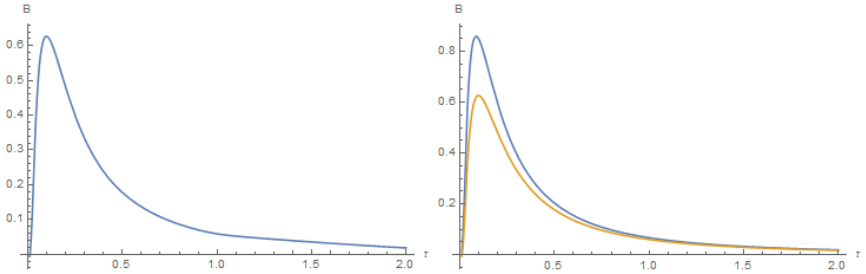

Figure 7: Right: Spectator contribution using Woods-Saxon Model (orange) and Hard-Sphere (blue) plotted together. As seen, both are within the order of magnitude window of 10^{18} Gauss which, in the realm of the strong fields produced as a result of heavy ion collisions, is close enough. Left : Spectator contribution to the magnetic field using Woods-Saxon Model in conductive medium.

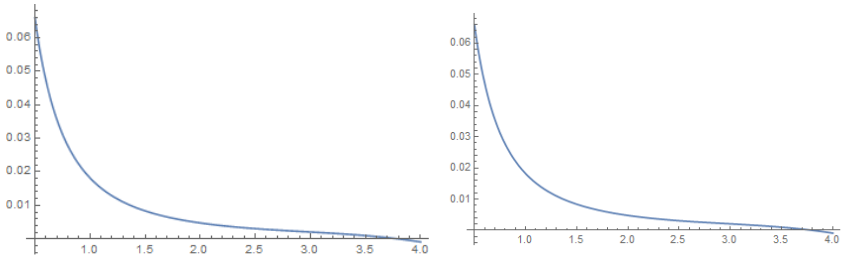

Figure 8: Left: Plot of the proper-time dependence of the magnetic field of the participants using the Woods-Saxon model. right: Plot of the proper-time dependence of the magnetic field of the participants using the Woods-Saxon model.

3.0.5 Participants contribution with Woods-Saxon Model

Figure 8 bellow shows the same contribution using the Woods-Saxon model. Again, the maximum value of the field is the same and about $0.065 fm^{-1}$ showing that the two models produce similar results in the case of the participants.

4 Discussion

In heavy-ion collisions, the nuclei pass each other at very high velocity. In these high energy situations, the confined matter inside the ions turns into the unconfined QGP. It is found that the relativistically moving heavy ions, typically with large positive charges, carry strong magnetic (and electric) fields with them. In the short moments before/during/after the impact of two ions in off-central collisions, there is a very strong magnetic field in the reaction zone. In fact, such a magnetic field is estimated to be of the order of 10^{18} Gauss, probably the strongest magnetic field in the present universe [15]. Since the distances between the nucleons are very small (i.e. very close to the reaction time and shortly afterwards), one would expect that the magnetic field of such reactions is very high. As argued by [14], observation of Lepton polarization can prove the existence of such strong fields in heavy-ion collision experiments.

In this study, we employed a semi-analytical model taking relativistic heavy ions as two Lorentz-contracted spheres of charge densities described by two different models. Ignoring interactions of particles we have then compared the resulting magnetic field obtained as a function of proper time. In our results we obtained the spectator contribution to the field which at its maximum has the strength of about 1.7×10^{18} Gauss using the Hard-Sphere model and 1.2×10^{18} Gauss for the Woods-Saxon model. We have also shown that the contribution to the field from the participants is negligible and that taking into account the conductivity, the field decays much slower.

Finally, we have argued that our results using the Woods-Saxon model match; in order of magnitude and up to statistical fluctuations, to results obtained using the approximation of a homogeneously-charged sphere by [1] , [13]. Therefore, we conclude that due to its simplicity, the Hard-Sphere model for charge distribution is a good-enough approximation when calculating electromagnetic fields in heavy ion collisions.

5 Potential topics for Further research

As we have seen, an enormous magnetic field can indeed be created in off-central heavy-ion collisions. At this point, a topic for further research could be:

We have seen that the magnitude of the created magnetic field drops as a function of proper time. This change in the magnetic field induces an electric field circulating around the direction of B_y by Faraday's Law. This electric field in turn creates a current which again induces an electric field in the z direction by the Lenz rule. Study of the effects of these inductions on the evolution of the colliding system is an interesting topic for further research (see also [14]).

Acknowledgment

I wish to thank Prof. Fatemi at the Physics department of Bahonar University in Kerman for directing me in the re-editing process.

References

[1] Gursoy, Umut and Kharzeev, Dmitri and Rajagopal, Krishna, 2014, Physical Review C, 89, 5

[2] Müller, Berndt and Schukraft, Jürgen and Wysłouch, Bolesław, 2012, Annual Review of Nuclear and Particle Science, 62, 361-386

[3] Greif, Moritz and Greiner, Carsten and Xu, Zhe, 2017, archive , arXiv:1704.06505,

[4] Boissé http://cerncourier.com/cws/article/cern/53089

[5] Zhong, Yang and Yang, Chun-Bin and Cai, Xu and Feng, Sheng-Qin, 2014, Advances in High Energy Physics

[6] Wong, Cheuk-Yin, 1994,World scientific

[7] Marcus, Eric, 2015

[8] Kharzeev, Dmitri E and McLerran, Larry D and Warringa, Harmen J, 2008, Nuclear Physics A, 803, 3-4, 227-253

[9] Kharzeev, D, 1996,Physics Letters B, 378, 1-4

[10] Schukraft, Jurgen and Stock, Reinhard, 2015, arXiv preprint arXiv:1505.06853

[11] Widrow, Lawrence M and Ryu, Dongsu and Schleicher, Dominik RG and Subramanian, Kandaswamy and Tsagas, Christos G and Treumann, Rudolf A, 2012, Space Science Reviews, 166, 1

[12] Allday, J, 2002

[13] McLerran, L and Skokov, V, 2014, Nuclear Physics A, 929, 184-190

[14] Tuchin, Kirill, 2010, Physical Review C, 82, 3

[15] Grasso, Dario and Rubinstein, Hector R, 2001, Physics Reports, 384, 3

[16] Duncan, Robert C and Thompson, Christopher, 1992, The Astrophysical Journal, 392, L9–L13

[17] URL: http://cerncourier.com/cws/article/cern/53089

[18] Foka, Panagiota and Janik, Małgorzata Anna, 2016, Reviews in Physics, 1, 154–171

[19] Bjorken, James D, 1983, Physical review D, 27, 1, 140

[20] Deng, W.T. and Huang, X.G., 2012, Physical Review C, 85(4), p.044907.

[21] Tarafdar, S. and Singh, V.

[22] ALICE collaboration and others, 2014, Physics Letters B, 734, 314–327,

[23] Patra, BK and Alam, Jan-e and Roy, Pradip and Sarkar, Sourav and Sinha, Bikash. and Singh,2002, Nuclear Physics A, 709

[24] De Jager, CW and De Vries, H and De Vries, C, 1974, Atomic data and nuclear data tables, 14, 5-6